J Mol Model (2018) 24: 268
https://doi.org/10.1007/s00894-018-3778-5

ORIGINAL PAPER

Cycloaddition reactions of pristine and endohedral fullerene molecules: possible anticancer activity

Jorge Gutiérrez-Flores[1] · Alfredo Moreno[1] · Francisco J. Vázquez[1] · Citlalli Rios[1] · Betzabeth Minutti[1] · Guadalupe Morales[1] · Aura Suarez[1] · Estrella Ramos[1] · Roberto Salcedo[1]

Received: 14 March 2018 / Accepted: 1 August 2018 / Published online: 1 September 2018

Abstract

Epoxide of oestradiol is one of the main risk factors for the genesis and evolution of breast cancer; hence, in recent years there has been considerable interest in the investigation of new inhibitors capable of reducing its carcinogenic activity. The aim of this article is to study the [2+2] cycloaddition reaction of epoxide of oestradiol in different pristine (C_{76} and D_{5h}-C_{80}) and endohedral metallofullerene ($C_{72}@Sc_2C_2$, $C_{76}@Sc_2$ and $C_{80}@Sc_2$) by means of molecular electrostatic potential (MEP) topological analysis. Different from other molecular scalar fields, MEP topology enables to find minima related to lone pairs and π electrons, therefore, this molecular scalar field is appropriate to identify the most reactive sites. In consonance with our results, it was found that C_{80} was the best candidate to carry out the epoxide of oestradiol cycloaddition since more stable adducts were obtained. Furthermore, it is expected that more than one oestradiol epoxide molecule will be added to C_{80}, forasmuch as C_{80} reactivity is enhanced once the adduct is formed. The study was carried through DFT framework included in the Gaussian 09 package (MPWB95/6-31G(d,p)).

Keywords Cycloaddition reactions · Theoretical calculations · Endohedral complexes

Introduction

Cycloaddition reactions between organic substances are known procedures that are carried out in the presence of UV radiation [17]. Nevertheless, the corresponding thermal procedure does not yield any products since, according to the Woodward–Hoffman rules [35], the symmetry of the orbitals is not appropriate for the attack. However, the elevated energy provided by the photoreactive method allows the reactants to reach a level in which the symmetry of the orbitals is propitious for the addition.

Despite the aforementioned, there are several recent reports indicating that this kind of procedure is possible in both pristine and endohedral fullerenes [23–25, 39, 40] because the frontier molecular orbitals of these systems have sufficient symmetry to permit [2+2] cycloaddition. Indeed, this procedure is the source of several interesting derivatives of fullerene, which have important applications [7, 20].

Endohedral fullerenes are derivatives in which many different guest species are found in the space within the cages of the fullerene [29]. A clear preference for large fullerenes (C_{80}, C_{82}, etc.) as hosts has been observed, while the guests can be free elements (mainly alkaline, lanthanide or actinide metals) [29, 33], small molecules such as nitrides, carbides, and oxides [38]. It is even possible to contemplate a fullerene fitting within one another, in a structure that resembles a Matryoshka doll [4].

Due to biocompatibility of nanometer-scale carbon structures and low toxicity [14], fullerene biomedical applications are of great interest [6, 22]. In previous reports, our group has demonstrated that pristine fullerenes can work as electron acceptors of oestradiol epoxide (which is one of

Electronic supplementary material The online version of this article (https://doi.org/10.1007/s00894-018-3778-5) contains supplementary material, which is available to authorized users.

✉ Roberto Salcedo
salcedo@unam.mx

[1] Instituto de Investigaciones en Materiales, Universidad Autónoma de México, Circuito Exterior s/n, Ciudad Universitaria, Coyoacán, Mexico City, 04510, Mexico

the main risk factors for the genesis and evolution of breast tumours [28]), decreasing its reactivity and avoiding its carcinogenic activity [30, 31]. We have also suggested that fullerene C_{60} can account to inhibit the carcinogenic activity of this oestrogen agent. The main contribution of fullerene in those cases was due to the electronic interchange between fullerene and the terminal groups of oestradiol.

Considering the above mentioned, the aim of this work is to study the interaction between bigger pristine fullerenes (C_{76} and D_{5h}-C_{80}) and endohedral metallofullerenes ($C_{72}@Sc_2C_2$, $C_{76}@Sc_2$ and $C_{80}@Sc_2$) with oestradiol epoxide. As these systems show a different electronic distribution of the frontier molecular orbitals from C_{60}, it is expected that exploring this new possibility would allow us to propose these structures as new and potential agents for the prevention of breast cancer.

Methods

In order to recognize the possible sites where [2+2] cycloaddition reactions can occur, a topological analysis of the molecular electrostatic potential (MEP) was carried out in the fullerenes of interest. As distinct from other molecular scalar field for (like electron density and electron localization function), MEP can be used to identify both structural and electronic features of molecules [19]. In addition, by means of the topological analysis of MEP, it is possible to find minima related to lone pairs and π electrons ((3,+3) critical points), which are absent in other scalar fields [19]. Considering the information provided by MEP and the subsequent molecular and topological analysis, different cycloaddition reactions have been described [3, 5, 16, 26].

In order to estimate the energy involved (ΔH) in the cycloaddition reactions, the following expression was employed:

$$\Delta H = H_{full-est} - \left(H_full + H_{est}\right) \quad (1)$$

Where H's represent the enthalpies of reactants (H_{full} and H_{est} for each fullerene and epoxide of oestradiol, respectively) and products ($H_{full\text{-}est}$) participating in the [2+2] cycloaddition reactions. An example of this reaction is shown in Fig. 1. Some properties related to all MEP minima (its value, number of electrons and volume), as well as the ΔH's for each possible reaction site of the fullerenes of interest are shown in Tables S1, S2, S3, S4 and S5 in SI. Graphic representations of the MEP minima are shown in Figs. S1, S2, S3, S4 and S5 in SI.

Furthermore, a geometrical analysis for each possible reaction site for all of the studied fullerenes was made by means of the π-orbital axis vector (POAV) analysis, which enables to describe the electronic structure of nonplanar conjugated organic molecules [11, 12, 14] via the atoms coordinates. Through this analysis, we determined the pyramidalization angle (θ_P), the s content of the π-orbital (m) and the p content of the σ-orbitals. Results for every possible site are in Tables S6, S7, S8, S9 and S10 in SI.

All calculations were carried out by means of Density Functional Theory (DFT) framework [15, 18], the MPWB95 [41, 42] functional (which has proved to give a good approach for covalent and noncovalent thermochemistry [41]) and the 6-31G(d,p) basis set (MPWB95/6-31G(d,p)), both included in Gaussian 09 package [1]. Geometry optimization processes were performed for the oestradiol epoxide molecule, both pristine and endohedral fullerenes and for every possible product from the [2+2] cycloaddition. Frequency calculations were made at the same level of theory in order to confirm that the optimized structures were at the minimum of the potential surfaces. Furthermore, from vibrational frequency calculations, corrections to the energy by translational, rotational and vibrational contributions at standard temperature (298.15 K) and pressure (1 atm) were obtained. The topological analysis of the MEP was achieved through Multwfn software [21].

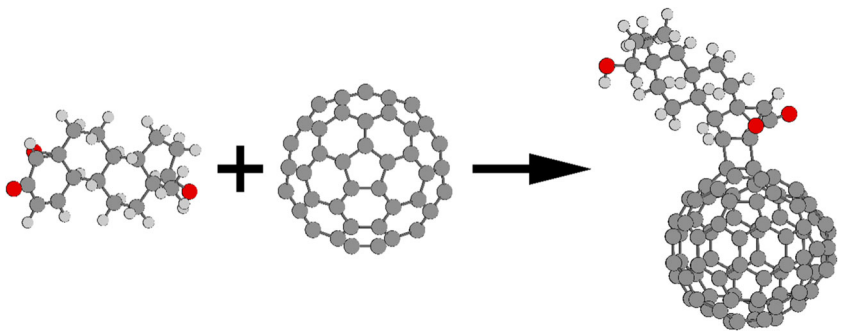

Fig. 1 Example of a [2+2] cycloaddition reaction for C_{80} with epoxide of oestradiol

Results and discussion

The studied species, pristine and endohedral fullerenes and epoxide of oestradiol molecule, are shown in Fig. 2. It can be seen that there are many possible fullerene sites where the cycloaddition of the epoxide of oestradiol is likely to occur. Therefore, it is necessary to use a descriptor capable of shedding light and show us the most favorable sites where the reaction can be carried out.

Regioselectivity of fullerenes is mainly determined by two factors: the configuration and distribution of both pentagonal and hexagonal rings, and the presence of molecules or atom clusters inside of it. The loss of electronic resonance and the deformation of the rings produce different tension values and forced angles. These phenomena lead to the existence of non-equivalent bonds in which cycloaddition reactions could be possible [36], whereas the presence of a metallic cluster inside the fullerene produces a charge transfer towards the outer part of the structure. Moreover, depending on its internal position, the cluster can contribute to a greater tension of bonds, causing the reactivity of the fullerene either increase or decrease [37]. In order to analyze these effects, Garcia-Borràs and coworkers defined the additive local aromaticity (ALA) index [8]. This is adequate to describe and predict the stability of endohedral metallofullerenes and is convenient to find the reactive sites by means of the local aromaticity. However, this index is useful only for endohedral fullerenes.

The geometrical and electronic features mentioned above have an important effect on the electronic distribution. Consequently, the study of the regioselectivity by means of the molecular electrostatic potential (MEP) will show the most propitious sites in fullerenes where the [2+2] cycloaddition reactions can be achieved for both pristine and endohedral fullerenes.

Different from other scalar fields, (3,+3) critical points (minima) can be obtained from the topological analysis of MEP. These (3,+3) critical points, known as repulsors are associated to the presence of lone pairs and π electrons throughout a given structure [19]. Hence, the topological analysis of MEP was used in this work in order to detect the possible sites where the cycloaddition of epoxide of oestradiol could be carried out, in both pristine and endohedral fullerenes. All sites where these minima were found, for each pristine and endohedral studied fullerenes, are shown in Tables S1, S2, S3, S4 and S5 in SI. The possible formation of adducts in all of the sites where a minimum was found was also studied. The energy formation (ΔH) for the products in each site for every fullerenes is shown in Tables S1, S2, S3, S4 and S5 in SI.

Based on topological analysis of MEP, it was found that the most stable formed products correspond to those produced from C_{76}, $C_{76}@Sc_2C_2$ and C_{80} (see Tables S1, S2, S3, S4 and S5 in SI). However, C_{80} has more favorable sites than C_{76} and $C_{76}@Sc_2$, since a greater amount of stable adducts were formed.

In order to understand the difference in the reactivity of each fullerene, an inspection of the frontier molecular orbitals (FMO) was performed. This analysis is shown in Fig. 3 and it can be observed that the difference in energy between the HOMO of fullerene and the LUMO of epoxide of oestradiol ($\Delta E_{HOMO_{full}-LUMO_{est}}$) and LUMO of fullerene and HOMO of epoxide of oestradiol ($\Delta E_{LUMO_{full}-HOMO_{est}}$) is similar for every pristine and endohedral fullerene. However, the smallest differences in energy were found for C_{76}, $C_{76}@Sc_2$, C_{80} and $C_{80}@Sc_2$ $\Delta E_{LUMO_{full}-HOMO_{est}}$. With exception of $C_{80}@Sc_2$, the results obtained from the FMO analysis are in good agreement with those of MEP topology, where C_{80}'s $\Delta E_{LUMOfull\text{-}HOMOest}$ is the smallest difference and therefore, C_{80} the molecule with the most stable adducts. With respect to $C_{80}@Sc_2$, the reason why no stable cycloaddition products were formed could be associated to the shape of molecular orbitals (they are different from those of HOMO of epoxide of oestradiol, consequently the reaction can not occur). These results are consistent

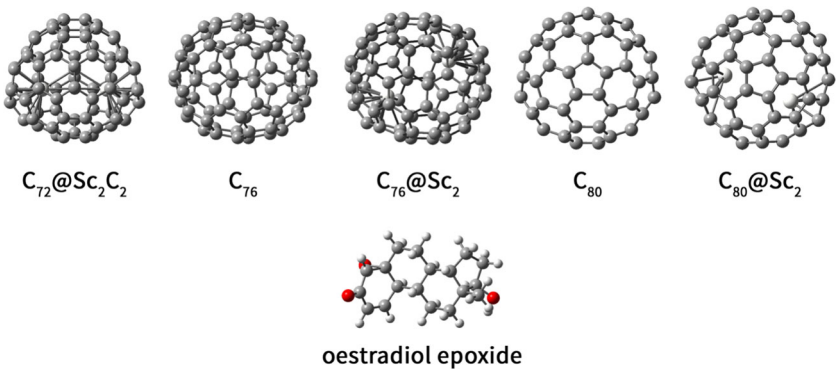

Fig. 2 Representation of studied species, pristine and endohedral fullerenes and epoxide of oestradiol molecule

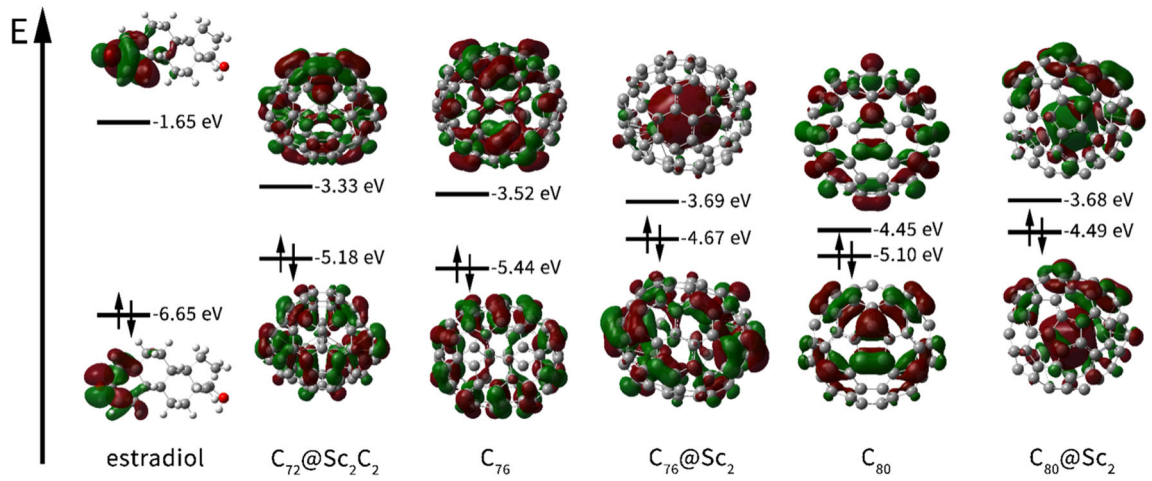

Fig. 3 FMO diagram of the interaction between epoxide of oestradiol molecule and the different studied fullerenes

with previous works, where studied fullerenes behaved as electron acceptors of epoxide of oestradiol [30, 31].

As was mentioned before, both the distribution of pentagonal and hexagonal rings and the presence of metal clusters inside the fullerene have an effect on the electronic distribution. These effects can be observed in the HOMO of C_{76}, C_{76}@Sc_2, C_{80} and C_{80}@Sc_2, where the electronic distribution changes, together with the distribution of the rings and the presence of metals inside the fullerenes. To make these effects more visible, the molecular electrostatic potentials and the dipole moments are shown in Fig. 4.

In the case of C_{76} and C_{76}@Sc_2, the effect of the presence of scandium atoms is remarkable (see Fig. 4). While in the pristine fullerene, the charge distribution is uniform ($\mu = 0$ D), in C_{76}@Sc_2 the electron density tends to polarize ($\mu = 0.8246$ D), increasing the sites where stable adducts can be formed (see Tables S2 and S3 in SI). The presence of scandium atoms also has an important effect on the molecular orbital energies, as scandium atoms donate electrons to the LUMO of pristine fullerene, the energy of HOMO increases but the energy of LUMO tends to decrease (see Fig. 3), increasing the capacity of endohedral fullerene to accept electrons derived from epoxide of oestradiol and to obtain more stable products once the cycloaddition is carried out (see ΔH's in Tables S2 and S3 in SI). In contrast, the presence of scandium atoms in C_{80}@Sc_2 reduces its reactivity (see Tables S4 and S5 in SI), since the polarizability decreases when scandium is added to the pristine fullerene ($\mu = 0.5792$ D for C_{80} and $\mu = 0.5422$ D for C_{80}@Sc_2, for a better overview see Fig. 4) and both HOMO and LUMO increase their energy.

Distribution of pentagonal rings has a direct effect on fullerenes shape [32]. Comparing pristine fullerenes, C_{76} exhibits a lower associated reactivity associated than C_{80} due to its regular charge distribution (see Fig. 4). Since pentagonal rings are more homogeneously distributed in C_{76} whereas in C_{80} are more concentrated in an specific zone (see Figs. 2 and 4). These results suggest that pentagonal rings are responsible for the polarization of electron density. Consequently, the reactivity of fullerenes

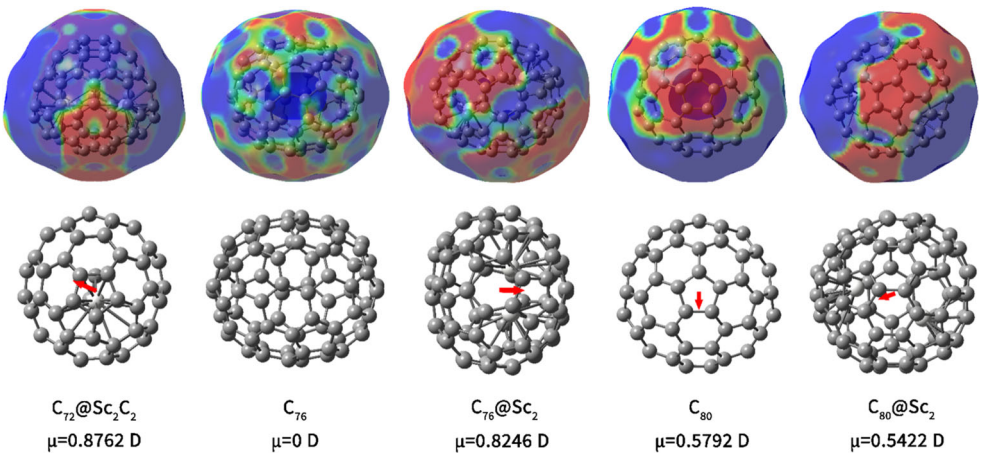

Fig. 4 Molecular electrostatic potentials (MEP) and dipole moments μ (represented by *red arrows*) of pristine and endohedral fullerenes. *Red zones* in MEP represent minima, while *blue zones* represent maxima

will be associated to pentagonal rings distribution. This is also reflected in MEP minima arrangement. Based on the above mentioned, as pentagonal rings are more distributed along C_{76} structure several minima were found in MEP topological analysis (see Fig. S2 and Table S2 in SI) and, as each MEP minima withdraws electron density, the charge distribution in this molecule will be uniform (this is the reason why dipole moment is null). On the contrary, a lower amount of minima in topological analysis of MEP (see Fig. S4 and Table S4 in SI) and a dipole moment different from zero were found in C_{80}, since pentagonal rings are less distributed along fullerene structure, therefore increasing its reactivity. This analysis is consistent with that reported by other authors [9, 13, 34].

A geometrical examination through the π-orbital axis vector (POAV) analysis was made for each reaction site for each pristine and endohedral fullerene (results are shown in Tables S6, S7, S8, S9 and S10 in SI). By means of POAV analysis, the pyramidalization angle (θ_P), the s content of the π-orbital (m) and the p content of the σ-orbitals were determined for each atom involved in [2+2] cycloaddition. No relationship was observed between θ_P, m and n with the tendency to form stable adducts. Nevertheless, it is clear that each site involved in the cycloaddition has a θ_P greater than 10° and an important sp^3 character.

To get a better idea of how geometrical features contribute to reactivity, a deeper analysis was carried out for C_{80}, since a greater amount of stable products was obtained from this compound. In Table 1 the energies of the most stable adducts are shown. It can be noticed that most of reactive sites correspond to [5,6] bonds. As previously mentioned, the reactivity of fullerenes is associated with the presence of pentagonal rings. Hence, it is concluded that the most stable adducts correspond to those where a pentagonal ring is present. In fact, the most stable product was obtained in a [5,6] bond (see Table 1).

As shown, the [6,6] bond reported in Table 1 is surrounded by pentagonal rings. Therefore, in spite of not directly involving a pentagonal ring, a stable product can be formed. The influence of pentagonal rings over the reactivity of [6,6] and [5,6] bonds can be observed in Table 2, where the mean pyramidalization angles ($\bar{\theta_P}$) of most reactive sites (where the most stable adducts were obtained) are shown. Additionally, a site where no minima were found in topology of MEP, was added in order to make comparisons (the last one in Table 2). When a pentagonal ring is involved in the reaction site (either as part of the bond or as part of the bond neighborhood), $\bar{\theta_P}$ tends to increase and reactivity is enhanced. In the case of [6,6] bond where carbon atoms number 8 and 9 are involved, only hexagonal rings are surrounding this bond, resulting in a lower $\bar{\theta_P}$ and a poor reactivity (no minima was found in this bond).

In order to study the adducts' stability, in Fig. 5 the FMO and charge distribution analysis are shown for the most stable product. It can be seen from FMO analysis that neither the HOMO nor the LUMO of [5,6] product are involved in the formed bonds from the cycloaddition; these results indicate that the adduct is stable. On the other hand, it can be inferred from Fig. 5 that electrons are donated from epoxide of oestradiol to C_{80}, since the energy difference of C_{80}'s HOMO and [5,6] product's HOMO is relatively short. This is in agreement with the previous analysis. Starting with MEP analysis (Fig. 5), a greater charge distribution is observed when epoxide of oestradiol is added to C_{80}, i.e., the dipole moment is greater for the adduct than for the pristine fullerene. This may imply the ability of C_{80} to be involved in more cycloaddition reactions, i.e., once an epoxide of oestradiol molecule is added, the reactivity of C_{80} could be enhanced. This in an important issue for future research.

Finally, it is important to mention that most of the stable adducts in the different studied fullerenes were obtained when the cycloaddition was carried out in [5,6] bonds (see Tables S6, S7, S8, S9 and S10 in SI). Integrating the electron

Table 1 Energy formation (ΔH) of C_{80} most stable formed adducts

Site	Type	ΔH (kcal mol^{-1})
34,42	5,6	–0.01
34,38	5,6	–3.58
23,31	5,6	–0.55
56,64	5,6	–2.70
01,03	6,6	–0.77
67,75	5,6	–0.55
16,27	5,6	–2.37
27,72	5,6	–0.36

Table 2 Mean pyramidalization angles ($\bar{\theta_P}$) of C_{80} reaction sites associated with the most stable formed adducts

Site	Type	$\bar{\theta_P}$
34,42	5,6	10.24
34,38	5,6	10.80
23,31	5,6	10.57
56,64	5,6	10.71
01,03	6,6	11.96
67,75	5,6	10.56
16,27	5,6	10.80
27,72	5,6	10.80
08,09	6,6	7.46

The last site is not presented in Tables S4 and S9 due to no (3,+3) critical point was found, it was added in order to make comparisons

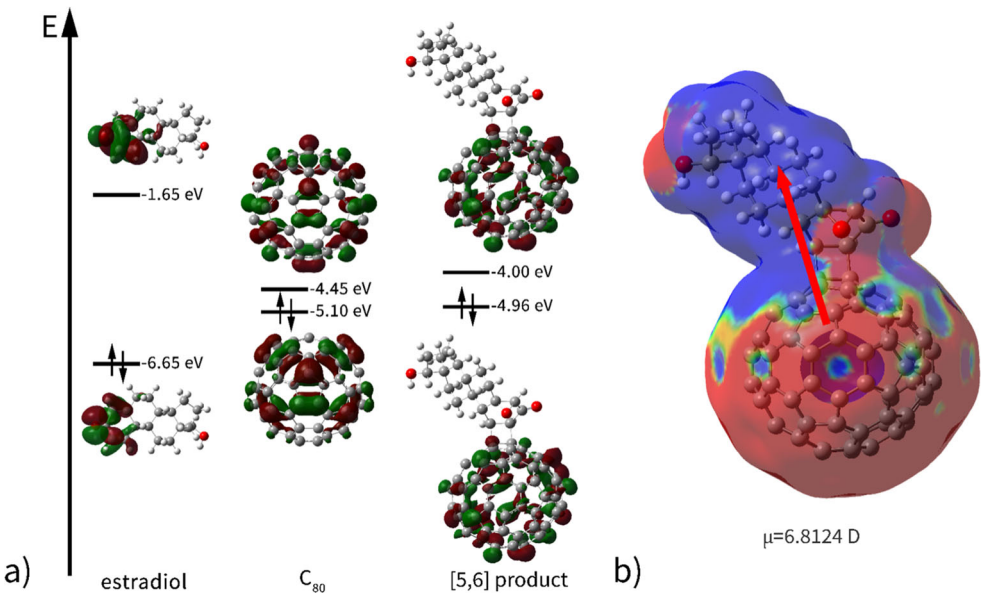

Fig. 5 **a** FMO diagram of the reaction between epoxide of oestradiol and C_{80}; molecular orbitals are also shown for the most stable adduct. **b** Molecular electrostatic potential (MEP) and dipole moment of the most stable adduct formed by the reaction between epoxide of oestradiol and C_{80}

density in the MEP basins, the average number of electrons related to (3,+3) critical points and the associated volume were obtained. It was found that, in general, the largest volumes are related to sites where the most stable products are formed (see Tables S6, S7, S8, S9 and S10 in SI). Therefore, the reactivity of fullerenes is enhanced when a greater amount of pentagonal rings are concentrated in a specific site or when a pentagonal ring is directly involved in the reaction site. Having the [5,6] as the best sites where the [2+2] cycloaddition can occur. This finding is in agreement with other studies made for pristine [27] and endohedral [2, 10, 39] fullerenes. Of the studied fullerenes, the best candidate to be employed as a possible treatment for breast cancer is C_{80}, since it showed to have the stable adducts and a greater number of sites where the epoxide of oestradiol cycloaddition can occur.

Conclusions

Different pristine (C_{76} and C_{80}) and endohedral metallofullerenes ($C_{72}@Sc_2C_2$, $C_{76}@Sc_2$ and $C_{80}@Sc_2$) were studied with the aim of determining the best candidate to react with oestradiol epoxide, by means of a [2+2] cycloaddition reaction. And subsequently propose new alternatives for breast cancer treatment. As many possible sites were found in fullerenes to carry out the [2+2] cycloaddition of epoxide of oestradiol, a topological analysis of the molecular electrostatic potential (MEP) was performed in order to identify the most propitious reaction sites, and geometrical parameters were also obtained. Taken together, these results suggested that the most reactive sites are those which have associated a (3,+3) critical point, originated by the pyramidalization in the structure, a consequence of the presence of pentagonal rings. Therefore, the most favorable sites are those corresponding to [5,6] bonds.

Topology of MEP and FMO analysis revealed that the most stable adducts correspond to those from C_{76}, $C_{76}@Sc_2$ and C_{80}. However, since more reaction sites were identified for C_{80} and it also originated the most stable adducts, this molecule revealed to be the best candidate to carry out the cycloaddition.

Furthermore, it is expected that C_{80} reactivity will be enhanced once an estradiol molecule is added; this makes it possible for more than one epoxide of oestradiol molecule to be added to C_{80}.

Acknowledgements The authors would like to thank Alberto López, Cain González, Alejandro Pompa, María Teresa Vázquez for their kind help, Oralia Espinoza for her technical assistance and to DGTIC-UNAM for their supercomputing services. Many thanks also to DGAPA-UNAM for the grants corresponding to DGAPA PAPIIT IN203816 and RN203816 projects.

References

1. Frisch MJ, Trucks GW, Schlegel HB, Scuseria GE, Robb MA, Cheeseman JR, Scalmani G, Barone V, Petersson GA, Nakatsuji H, Li X, Caricato M, Marenich A, Bloino J, Janesko BG, Gomperts R, Mennucci B, Hratchian HP, Ortiz JV, Izmaylov AF, Sonnenberg JL, Williams-Young D, Ding F, Lipparini F, Egidi F, Goings J, Peng B, Petrone A, Henderson T, Ranasinghe D, Zakrzewski VG, Gao J, Rega N, Zheng G, Liang W, Hada M, Ehara M, Toyota K, Fukuda R, Hasegawa J, Ishida M, Nakajima T, Honda Y, Kitao O, Nakai H, Vreven T, Throssell K, Montgomery JA Jr, Peralta JE, Ogliaro F, Bearpark M, Heyd JJ, Brothers E, Kudin KN, Staroverov VN, Keith T, Kobayashi R, Normand J, Raghavachari K, Rendell A, Burant JC, Iyengar SS,

Tomasi J, Cossi M, Millam JM, Klene M, Adamo C, Cammi R, Ochterski JW, Martin RL, Morokuma K, Farkas O, Foresman JB, Fox DJ (2016) n.d. Gaussian 09, Revision E.01, Gaussian, Inc., Wallingford CT

2. Alegret N, Chaur MN, Santos E, Rodríguez-Fortea A, Echegoyen L, Poblet JM (2010) Bingel-Hirsch reactions on non-ipr $Gd_3N@C_{2n}$ ($2n$ = 82 and 84). J Org Chem 75:8299–8302
3. Balanarayan P, Kavathekar R, Gadre SR (2007) Electrostatic potential topography for exploring electronic reorganizations in 1,3 dipolar cycloadditions. J Phys Chem A 111:2733–2738
4. Bing-she XU (2008) Prospects and research progress in nano onion-like fullerenes. New Carbon Mater 23:289–301
5. Burke LA (1985) Theoretical study of (2+2) cycloadditions. Ketene with ethylene. J Org Chem 50:3149–3155
6. Cheng C, Wang H (eds) (eds. 2016) Biomedical applications and toxicology of carbon nanomaterials. Wiley, Weinheim
7. Nakamura E, Isobe H (2003) Functionalized fullerenes in water. The first 10 years of their chemistry. Acc Chem Res 25:807–815
8. Garcia-Borràs G, Osuna S, Swartm M, Luis JM, Solà M (2013a) Maximum aromaticity as a guiding principle for the most suitable hosting cages in endohedral metallofullerenes. Angew Chem Int Ed 52:9275–9278
9. Garcia-Borràs M, Osuna S, Luis JM, Swart M, Solà M (2014) The role of aromaticity in determining the molecular structure and reactivity of (endohedral metallo)fullerenes. Chem Soc Rev 43:5089–5105
10. Garcia-Borràs M, Osuna S, Swart M, Luis JM, Echegoyen L, Solà M (2013b) Aromaticity as the driving force for the stability of non-IPR endohedral metallofullerene Bingel-Hirsch adducts. Chem Commun 49:8767–8769
11. Haddon RC (1986) Hybridization and the orientation and alignment of π-orbitals in nonplanar conjugated organic molecules: π-orbital axiz vector analysis (POAV2). J Am Chem Soc 108:2837–2842
12. Haddon RC (1988) П Electrons in three dimensions. Acc Chem Res 21:243–249
13. Haddon RC (1993) Chemistry of the fullerenes: the manifestation of strain in a class of continuous aromatic molecules. Science 261:1545–1550
14. Haddon RC (2001) Comment on the relationship of the pyramidalization angle at a conjugated carbon atom to the σ bond angles. J Phys Chem A 105:4164–4165
15. Hohenberg P, Kohn W (1964) Inhomogeneous electron gas. Phys Rev 46:B864
16. Kanh SD, Pau CF, Overman LE, Hehre WJ (1986) Modeling chemical reactivity. 1. Regioselectivity of Dels-Alder cycloadditions of electron-rich dienes with electron-deficient dienophiles. J. Am. Chem. Soc. 108:7381–7396
17. Klopman G (1974) Chemical reactivity and reaction paths. Wiley, New York
18. Kohn W, Sham LJ (1965) Self-consistent equations including exchange and correlation effects. Phys Rev 140:A1133
19. Leboeuf M, Köster AM, Jug K, Salahub DR (1999) Topological analysis of the molecular electrostatic potential. J Chem Phys 111:4893–4905
20. Li C-Z, Chueh C-C, Yip H-L, Ding F, Li X, Jen AK-Y (2013) Solution processible highly conducting fullerenes. Adv Mater 25:2457–2461
21. Lu T, Chen F (2012) Multiwfn: a multifunctional wavefunction analyzer. J Comp Chem 33:580–592
22. Martín N, Da Ros T, Nierengarten F (2017) Carbon nanostructures in biology and medicine. J Mater Chem B 5:6425–6427
23. Martín N, Altable M, Filippone S, Martín-Domenech A, Güell M, Solá M (2006) Thermal [2+2] intramolecular cycloadditions of fuller-1,6-enynes. Angew Chem Int Ed 45:1439–1442
24. Mehta G, Viswanath M (1995) Novel bicyclo[2,2,0]hexane-fused [60]fullerene derivatives via cycloaddition with a cyclobutadiene diester. Tetrahed Lett 36:5631–5632
25. Mikie T, Asahara H, Nagao K, Ikuma N, Kokubo K, Oshima T (2011) Thermal [2+2] cycloaddition of morpholinoenamines with c_{60} via a single electron transfer. Org Lett 13:4244–4247
26. Murray JS, Yepes D, Jaque P, Politzer P (2015) Insights into Diels-Alder cycloadditions via the electrostatic potential and the reactions force constant. Comput Theor Chem 1053:270–280
27. Osuna S, Valencia R, Rodríguez-Fortea A, Swart M, Solà M, Poblet JM (2012) Full exploration of the Diels-Alder cycloaddition on metallofullerenes $M_3N@C_{80}$ (M=Sc, Lu, Gd): the d_{5h} versus i_h isomer and the influence of the metal cluster. Chem Eur J 18:8944–8956
28. Pasqualini JR, Chetrite G, Nguyen BL, Maloche C, Delalonde L, Talbi M, Feinstein MC, Blacker C, Botella J, Paris J (1995) Estrone sulfate-sulfatase and 17 beta-hydroxysteroid dehydrogenase activities: a hypothesis for their role in the evolution of human breast cancer from hormone-dependence to hormone-independence. J Steroid Biochem Mol Biol 53:407–412
29. Popov AA, Yang S, Dunsch L (2013) Endohedral fullerenes. Chem Rev 113:5989–6113
30. Pérez-Manríquez L, Ramos E, Rangel E, Salcedo R (2013) Interaction between epoxidised estradiol and fullerene (C_{60}): possible anticancer activity. Mol Simul 39:612–620
31. Rios C, Ramos E, Pérez-Manríquez L, Salcedo R (2014) Cycloaddition of oestrogen-like molecules on fullerene: theoretical approach. Mol Simul 41:1292–1297
32. Schwerdtfeger P, Wirz LN, Avery J (2015) The topology of fullerenes. WIREs Comput Mol.Sci 5:95–145
33. Shinohara H (2000) Endohedral metallofullerenes. Rep Prog Phys 63:843–892
34. Solà M, Mestres J, Duran M (1995) Molecular size and pyramidalization: two keys for understanding the reactivity of fullerenes. J Phys Chem 99:10752–10758
35. Woodward RB, Hoffmann R (1970) The conservation of orbital symmetry. Academic Press, New York
36. Yadav BC, Kumar R (2008) Structure, properties and applications of fullerene. Int J Nanotechnol Appl 11:15–24
37. Yamada M, Akasaka T, Nagase S (2010) Endohedral metal atoms in pristine and functionalized fullerenes cages. Acc Chem Res 43:92–102
38. Yang S, Liu F, Chen C, Jiao M, Wei T (2011) Fullerenes encaging metal clusters-clusterfullerenes. Chem Comm 47:11822–11839
39. Yang T, Nagase S, Akasaka T, Poblet JM, Houk KN, Ehara M, Zhao X (2015) (2+2) cycloaddition of benzyne to endohedral metallofullerenes $M_3N@C_{80}$ (M = Sc, Y): a rotating-intermediate mechanism. J Am Chem Soc 137:6820–6828
40. Zhang X, Fan A, Foote CS (1996) [2+2] Cycloaddition of fullerenes with electron-rich alkenes and alkynes. J Org Chem 61:5456–5461
41. Zhao Y, Truhlar DG (2004) Hybrid meta density functional theory methods for thermochemistry, thermochemical kinetics, and noncovalents interactions: the MPW1B95 and MPWB1K models and comparatives assessments for hydrogen bonding and van der Waals interactions. J Phys Chem A 081:6908–6918
42. Zhao Y, Truhlar DG (2005) Benchmark databases for nonbonded interactions and their use to test density functional theory. J Chem Theory Comput 1:415–432